Dehydration Enhances Prebiotic Lipid Remodeling and Vesicle Formation in Acidic Environments

Luke H. Steller,[†,¶] Martin J. Van Kranendonk,[†,¶] and Anna Wang[*,‡,¶]

†*School of Biological, Earth and Environmental Sciences, UNSW Sydney, Bedegal Country, NSW 2052, Australia*

‡*School of Chemistry, UNSW Sydney, Bedegal Country, NSW 2052, Australia*

¶*Australian Centre for Astrobiology, UNSW Sydney, Bedegal Country, NSW 2052, Australia*

E-mail: anna.wang@unsw.edu.au

Abstract

The encapsulation of genetic polymers inside lipid bilayer compartments is a vital step in the emergence of cell-based life. However, even though acidic conditions promote many reactions required for generating prebiotic building blocks, prebiotically-relevant lipids tend to form denser aggregates at acidic pHs rather than prebiotically useful vesicles that exhibit sufficient solute encapsulation. Here we describe how dehydration/rehydration (DR) events, a prebiotically-relevant physicochemical process known to promote polymerization reactions, can remodel dense lipid aggregates into thin-walled vesicles capable of RNA encapsulation even at acidic pHs. Furthermore, DR events appears to favor the encapsulation of RNA within thin-walled vesicles over more lipid-rich vesicles, thus conferring such vesicles a selective advantage.

Introduction

Protocells, the hypothetical precursor to the first biological cell, likely consisted of a self-replicating genome encapsulated within a membrane vesicle.[1] The membrane would have played key roles in protocell function, such as promoting prebiotic reactions,[2] protecting protocells from parasitic genetic material,[3] and defining an individual replicating unit that could potentially become capable of growth and division, Darwinian competition and subsequent evolution.[4,5]

One commonly-proposed class of lipid molecules that could have formed prebiotic membranes are fatty acids.[6] Fatty acids were abiotically available, produced from both exogenous sources such as meteorites[?] and endogenous sources such as Fischer-Tropsch-like synthesis on Earth.[7] Importantly, fatty acids spontaneously form vesicles when the pH of the solution is near the apparent pK_a of the fatty acid, for example between approximately pH 7-9 for decanoic acid.[6] The pH range for stability is determined by the fraction of carboxylic acid groups that are deprotonated, with complete protonation leading to formation of a neat oil phase and complete deprotonation leading to micelle formation.[8] Of all of the self-assembled structures possible, oligolamellar or thin-walled vesicles are the most effective structures for encapsulation because they have a semipermeable, contiguous membrane that delineates an internal aqueous volume. In contrast to dense lipid droplets or very multilamellar (or thick-walled vesicles), they also most closely resemble the cells of modern organisms.

The narrow pH range of vesicle stability constrains the environments in which fatty acid vesicles can form. Multiple studies have raised the conundrum that because fatty acid vesicles could not have formed in acidic conditions, then neither could life.[9,10] Many important prebiotic reactions, including RNA polymerization,[11] and nucleotide activation chemistry,[12] are optimised in acidic conditions. The Archean oceans are proposed to be acidic.[13] While mixtures of fatty acids with their corresponding alcohol or monoglyceride are capable of withstanding more alkaline conditions or higher salt concentrations,[14] fatty acid mixtures are generally observed to from dense oil droplets in acidic solutions,[15,16] unless prebiotically

implausible cationic lipids such as sodium dodecylbenzenesulfonate are used.[17] Recently, Bonfio *et al.* reported formation of a small fraction of decanoic acid:decanol:decanal (4:1:1) vesicles alongside oil droplets and aggregates in the presence of 100 mM 4,5-dicyanoimidazole (DCI) buffer at pH 5.5. What is still unknown is whether a vesicle phase can be strongly favored over oil droplets at low pHs, or indeed whether vesicle formation is even possible in the absence of high DCI concentrations.

In one previous study, Milshteyn and coworkers observed a 12-carbon fatty acid/monoglyceride system form vesicles in unfiltered hot spring fluids at pH 3.3.[18] While it is a proof of concept, a major cause of hot spring pool acidity is dissolved gases (e.g. SO_2 and CO_2), and thus fluid samples taken in the field can *de-gas* after collection.[??] Because vesicle imaging occurred up to six months from the time of sampling and were heated during imaging, it's highly likely that the pH of the vesicle solution when imaged had increased from the time of measurement in the field. Furthermore, the critical effects of dissolved salts[?] and organic materials[??] were not controlled for with the authors themselves stating that "an explanation is still uncertain". In this current study we take a more controlled approach by monitoring the sample pH and using non-volatile acids, while using a significantly more selective RNA dye and controlling for dissolved matter, to better understand the system.

Here we exploit the non-equilibrium nature of fatty acid lipid assemblies,[19] and use dehydration/rehydration (DR) events to remodel dense lipid assemblies into vesicles possessing a large aqueous lumen. DR events are significant in prebiotic research because they may have been commonplace on exposed land surfaces on early Earth, ranging from micro-events induced by humidity[20] to larger events in daily tidal pools and even yearly weather patterns.[21] Hot springs are of particular interest as an environment capable of protocell production, as they not only display regular DR events on a range of time scales, but can capture meteor-delivered organics, concentrate prebiotically-essential elements, and were likely present on the early Earth's surface when life was forming.[22,23]

While DR events are known to enable encapsulation of solutes such as genetic material

into bilayer vesicles,[6,24,25] the ability of DR to favor certain vesicle topologies, or remodel membranes, has not been previously investigated. Recently Sankar *et al.* explored how multiple DR events (referred to as wet/dry cycles) affected bulk vesicle properties such as turbidity and dye encapsulation, demonstrating that lipid systems can undergo multiple DR events and still maintain their ability to form vesicles and encapsulate solutes.[26] In this work we focus on understanding the effect of DR events on remodelling prebiotically-plausible lipid mixtures at the individual vesicle level, leading to encapsulation of RNA. In particular, we use microscopy to glean insight into population heterogeneity rather than average properties of a bulk sample. By doing so, we demonstrate that a single DR event can remodel dense lipid aggregates into vesicles at acidic pH. Furthermore, by using a fluorescent dye that targets single-stranded RNA with excellent selectivity, we show that DR biases the encapsulation of RNA into vesicles that have thinner walls (oligolamellar), rather than thicker walls (very multilamellar). This demonstrates that DR events have the potential to not only remodel lipid into protocells at lower pHs, but it provides a selective advantage to vesicles that have an architecture more akin to modern cell membranes.

Results

Selective preference for RNA encapsulation within thin-walled vesicles over multilamellar vesicles

We initially examined vesicle formation of the well-accepted prebiotic mixture of decanoic acid and glycerol monodecanoate (DA and GMD) at a pH near the apparent pK_a of decanoic acid. In a system buffered with PBS (phosphate-buffered saline) to pH 7.4, vesicles spontaneously formed after slight agitation of lipid (30 mM DA:GMD, 1:1), as observed by brightfield (no phase ring) microscopy (Fig. 1A). We chose this pH to optimize vesicle formation by working near the apparent pK_a of the lipid mixture (approximately 7.5[15]). As expected, when yeast RNA (0.1 mg/mL) along with a fluorescent RNA dye QuantiFluor

was included in the buffer, no biased encapsulation was observed, as indicated by uniform fluorescence across the entire image (Fig. 1B). This is because without exposing the system to an encapsulation process, the RNA is evenly distributed throughout the sample.

We then subjected the DA:GMD and RNA aqueous system to a single DR event by evaporating to dryness *via* heat bath (90°C) then rehydrating with Milli-Q water to mimic a natural DR event by heat followed by hydration from rainfall or a hot spring geyser.

Upon rehydration, a range of different vesicle morphologies formed, including oligolamellar thin-walled vesicles, multilamellar thick-walled vesicles, and multilamellar onion-like vesicles. However, while most vesicles exhibited minimal RNA encapsulation relative to background, we observed that certain vesicle morphologies contained much higher concentrations of RNA (Fig. 1C,D).

To understand this uneven encapsulation better, we use two imaging modalities to investigate the observed bias in encapsulation. The broader encapsulation process has been reported in previous works, with Deamer & Barchfeld first proposing solute entrapment between lipid membranes during dehydration, then subsequent vesicles budding off during rehydration as a method of encapsulation.[24] In these previous studies, dyes used to visualize the RNA were cationic and thus also labelled the anionic fatty-acid-based membranes.[18] To confirm this, we tested a common RNA dye (Acridine Orange) at the amounts used in these previous studies and found that it readily labelled fatty acid vesicles even in the absence of RNA (Fig. S1). As a result, the localization of RNA as opposed to lipid could only be inferred indirectly when Acridine Orange and other cationic dyes were used.

Here we use a recently-developed RNA dye that selectively labels single-stranded RNA to better probe the system. Additionally, we exploit the fact that the variation in brightfield microscopy intensity corresponds to optical density (and by proxy, material density) to quantitatively distinguish between vesicle types in a label-free manner. Oligolamellar and multilamellar vesicles can be distinguished by measuring the intensity of light in a transect across the vesicle in brightfield microscopy and taking the standard deviation of intensity

across the transect (Fig. S2).

We find that when vesicle brightness is plotted against the standard deviation of vesicle intensity transects for each vesicle, there is a clear correlation between low membrane density (*i.e.* thin-walled vesicles) and RNA encapsulation (Fig. 1E). In other words, there is a clear trend of enhanced RNA encapsulation occurring almost exclusively within thin-walled vesicles, preferred over the thick-walled multilamellar vesicles, corroborated by the optical micrographs (Fig. 1C,D). While previous studies have observed that DR can lead to formation of vesicles that exclude RNA,[18,24] our results show that specific vesicle morphologies may in fact have the opposite behavior.

We also repeated our single DR event experiment with a well-known membrane label (Rhodamine B) and encapsulation marker (pyranine) instead of RNA. Again, we observed that the vesicles encapsulating the fluorescent pyranine dye were thin-walled (Fig. 2A–D), as confirmed by taking transects across the fluorescence images (Fig. 2E–F). Pyranine is clearly encapsulated within a lipid envelope (Fig. 2E), whereas lipid-dense vesicles encapsulate very little pyranine (Fig. 2F). These fluorescence microscopy results confirm that when biased encapsulation does occur, the vesicles with enhanced solute encapsulation are thin-walled vesicles rather than thick-walled. In other words, thin-walled vesicles are conferred an advantage by DR events.

Dehydration/Rehydration events remodel dense lipid aggregates into vesicles at a pH below their pK_{a}

The effects of a DR event were more profound at acidic pHs. When 30 mM of total lipid (1:1 DA:GMD) was added to an unbuffered solution of 10 mM NaCl and 0.1 mg/mL yeast RNA, the resulting pH was 5.4. Whereas an abundance of vesicles was observed under brightfield in the pH 7.4 system buffered with PBS, at pH 5.4 the lipid mixture formed liquid droplets that had a propensity to wet surfaces such as glass slides or plastic centrifuge tubes, indicative of their high surface energy. Under microscopy, emulsion droplets were dominant under

brightfield and no biased encapsulation was observed under fluorescence (Fig. 3A–B). These results are consistent with previous results, where a decanoic acid and decanol mixture was not able to form vesicles at pH 5.5[6,27] and a decanoic acid/decanal/decanol mixture was only observed to have a small fraction of vesicles present at pH 5.5.[12]

However, when we exposed our lipid system to a single DR event, the lipid droplets remodelled to form a diverse range of vesicles, similar to those observed in the pH 7.4 system. These remodelled vesicles were capable of encapsulating RNA in solution, again with enhanced encapsulation in thin-walled vesicles (Fig. 3C–F). No observable change was measured in the pH of the solution after rehydartion. This effect was confirmed in a buffered acidic system: When DA:GMD was mixed into 0.01 M citrate buffer (pH 5.3), it only formed dense lipid droplets. After one DR event, however, it formed a large range of vesicle morphologies (Fig. S4). We found that the lipid system buffered at pH 3.9 with 0.01 M citrate did not form vesicles upon rehydration, indicating a lower pH limit for the remodelling phenomenon (Fig. S4).

Finally, we confirm that although the remodelled vesicles are capable of encapsulating RNA present within solution, lipid remodelling is not driven by the specific chemical or ionic nature of the encapsulated molecules. This phenomenon was replicated using an uncharged encapsulation material (sucrose) as well as no additional encapsulation material present. In both instances, dense lipid aggregates were able to be remodelled into thin-walled vesicles after rehydration (Fig. S5, S6).

Discussion

Our research presents evidence for a purely-physical remodelling method to form fatty acid vesicles, enabling increased encapsulation inside oligolamellar vesicles even at acidic pHs. Because heating was used to accelerate dehydration in our experiments, we questioned whether heat itself was driving the remodelling, as previous work has noted that elevated tempera-

tures can cause temporary phase transitions (*i.e.* melting) for both phospholipids[28] and fatty acids[29,30] that lead to vesicle formation at higher temperatures. However, this is a transient effect, as vesicles formed in these systems transform back into dense lipid droplets or crystals once the temperature is reverted back to room temperature. Despite DA and GMD being solids at room temperature, a 1:1 combination of the two results in a mixture that is a liquid at room temperature (Fig. S7). This eliminates lipid heating as a primary driver for vesicle remodelling in this system, because the fatty acid mixture is already a liquid at room temperature. This was confirmed experimentally when pH 5.4 DA:GMD solution is dried down with passive evaporation at room temperature (∼22°C), the lipid is still remodelled to form vesicles similar to those formed after drying at elevated temperatures (Fig. S8).This vesicle system is stable for long time periods after initial remodelling, still containing thin-walled vesicles nearly 11 months after first forming them (Fig. S9). Regardless of drying temperature, the vesicles produced by our method are stable at room temperature, demonstrated by all vesicles microscopy images being captured at ∼22°C. We can therefore rule out heat itself as a driver for lipid remodelling.

While heat isn't a major factor in these experiments, the dispersal of lipid within an aqueous solution is crucial for lipid remodelling to occur. Lipids are commonly dissolved non-aqueous solvents as a first step towards creating vesicles.[31,32] However, when a DA:GMD mixture was added to methanol instead of water or aqueous buffer and then dried down, only emulsion droplets were observed upon rehydration (Fig. S10). Methanol is an excellent solvent for the lipids, and therefore does not promote any lipid self-assembly. Removal of methanol by dehydration simply leads to oil droplets forming, with lipid molecules arranged in an amorphous . By contrast, water is a poor solvent for the lipids and thus attempts at dispersing the lipids into aqueous solution result in lipids interacting pre-organizing *via* hydrogen bonding and hydrophobic forces.

Proposed Model for Membrane Remodeling

We imaged lipid before and after a dehydration event to determine what type of restructuring takes place. The DA:GMD mixture forms an oil that is immiscible with water and spreads as a droplet on the microscope slide (Fig. S11). Upon mixing with a simple 10 mM NaCl solution and subsequent dehydration without rehydration, complex heterogeneous structures formed. These include layered lipid structures showing birefringence under crossed polarizers, and halite crystals incorporated in lipid aggregates (Fig. S11). This suggests that physical restructuring and pre-stacking of lipid is contributing to lipid remodelling upon rehydration.

We propose two separate effects that are promoting lipid remodeling and encapsulation of solutes into oligolamellar vesicles: increased concentration of salts during dehydration, and osmotically-driven swelling of lipids during rehydration (Fig. 4).

During dehydration, solutions are concentrated and thus the ionic strength increases with time. Interestingly, the apparent pK_a of fatty-acid based vesicles depends on ionic strength. Maeda *et al.*[33] reported salt-dependence in the titration curve of oleic acid, with the apparent pK_a decreasing by 0.7 upon an increase in ionic strength from 10 mM NaCl to 100 mM NaCl. Mele *et al.*[34] modeled that the apparent pK_a for oleic acid decreases by 2.2 upon an increase in ionic strength from 1 mM NaCl to 150 mM NaCl. This behavior is predicted by the Poisson-Boltzmann equation. In brief, charged surfaces such as fatty acid bilayer membranes recruit counterions, including protons, reducing the pH of the surface. The apparent pH at the bilayer surface is thus lower than the bulk pH, leading to an increase in the apparent pK_a of the fatty acid. An increase in salt concentration decreases the efficiency of proton recruitment to the interface, leading to a smaller apparent pK_a shift. Thus, as the solution evaporates, we expect the apparent pK_a of the lipid to decrease to lower pHs. If the pH of the sample decreases minimally or stays constant owing to buffering agents, the deprotonation of the membrane is expected to increase with evaporation, thereby favoring lipid deprotonation (Fig. 4A). The negatively charged carboxylate residues can then interact more strongly with cations such as sodium ions, hereby forming pre-organized lipid layers

upon further dehydration (as shown in Fig. S11). Upon rehydration with water, bilayer structures may be able to form more readily from these pre-organized sheets than from homogeneous oil droplets, leading to an increase in vesicles as opposed to dense oil droplets.

During rehydration, there is a large osmotic driving force for pre-organized lipids that are co-localized with solute to be hydrated. The rate of lipid swelling and vesicle formation is then determined by water permeation across the membrane. The flux of water J across the lipid is related to the solute concentration difference across the membrane Δc by $J = P\Delta c/n$ where P is the permeability of water across a single bilayer, and n is the number of bilayers across which water needs to permeate. When solute is trapped underneath a thick layer of lipid, water permeates slowly and the lipid film swells at a slower rate. Conversely, when pockets of solute are trapped underneath a thin layer of lipid, water is able to readily permeate across the lipid layers and swell the film, leading to the formation of solute-rich oligolamellar vesicles (Fig. 4B).

Origin of Life Implications

This research provides new insight into the environmental conditions suitable for forming life on Earth. Our findings open up new regions of geochemical parameter space, creating the potential for prebiotically plausible vesicles to form in acidic conditions, making encapsulation accessible to chemical reactions that favour lower pH environments (*e.g.* RNA polymerization).[2]

Furthermore, DR appears to confer advantage to thin-walled protocells owing to their increased encapsulation of prebiotically useful macromolecules relative to other vesicle types. These oligolamellar vesicles are closer in morphology to the unilamellar membranes that encapsulate modern cells,[35] and may also be more prebiotically preferable due to their increased permeability.[36] This is because membrane permeability is an important feature in biology, with cells possessing pumps and pores to allow the exchange of material. Multilamellar thick-walled vesicles would have been a disadvantage for early protocells, restricting

the exchange of food and waste with the surrounding environment.[1] A protocell formation process that biases encapsulation of solutes into thin-walled vesicles, which are relatively permeable and readily exchange material with their environment, could have been extremely advantageous. Although this study focused on the effects of a single dry-down event, it has been clearly shown in other studies that fatty acid vesicle systems can undergo multiple DR events and still maintain their ability to form vesicles and encapsulate solutes,[26] increasing its suitability as a potential prebiotic protocell system.

Lastly, our findings highlight that special attention should be given to the method of vesicle formation and hence path of lipid assembly when comparing results from different studies. This is because while prebiotically-plausible lipids are vastly more soluble and their assemblies more dynamic their than phospholipid counterparts, prebiotic lipid systems are still capable of being kinetically-trapped and are not true equilibrium systems.[37] In the origins of life field, researchers use a range of vesicle preparation methods such as titration,[38] thin film hydration,[9] and wet/dry cycling with varying surfaces and solvents,[18,39] with and without shear[35] such as extrusion. These different methods can have a substantial effect on the resulting vesicle characteristics, as they are well-known to do for phospholipids.[40] While this provides exciting opportunities to the variety of different membrane-bound architectures that may have been present on early Earth, it also necessitates care when comparing vesicles produced by different methods.

Experimental

Reagents

10 mg/mL RNA solution (Ribonucleic acid from torula yeast, Type VI, Sigma-Aldrich): 100 mg of Yeast RNA was added to 10 mL of 10 mM EDTA solution (ChemSupply Australia) in Milli-Q water. The RNA solution was adjusted to pH 6 with 5 M NaOH (Lowy Solutions). QuantiFluor RNA System (Promega) was used as the RNA dye; other dyes used include

1 mM pyranine (Sigma-Aldrich) as an encapsulation marker, 0.1mM Acridine Orange to demonstrate its ability to label lipid, and 5 μm Rhodamine B (Sigma-Aldrich) as a membrane dye. Sucrose (ChemSupply Australia) made to 0.1 M was also used as a neutral encapsulation molecule. Buffers used include 1X PBS made from 10X PBS stock solution (Lowy Solutions), and 0.01 M citrate buffer (ChemSupply Australia), with pH adjusted with 5 M HCl (Lowy Solutions). 10 mM NaCl solutions were made by appropriate dilution of 5 M NaCl solution (Lowy Solutions). pH was measured using an Orion Star A121 pH Meter with a Orion 8103BN ROSS probe.

Vesicle preparation

All reagents for each specific experiment, including the appropriate lipid, encapsulation solutes, and buffers, were added to the Eppendorf tube, vortexed for 15 seconds, then agitated by scraping the tube three times against a microcentrifuge rack ('rumble-stripped'[41]). Tubes selected for dehydration were then partly-submerged in a heat bath (90 °C) for 1 hour. For analysis, dehydrated samples were rehydrated with 100 μL of Milli-Q water directly before analysis. Both samples (dehydrated and non-dehydrated) were rumble-stripped 5 times before microscope analysis to distribute vesicles through sample fluid and ensure representative selection of vesicles. Experiments were repeated on three separate occasions, with consistent results recorded in each replication.

Imaging

Images were captured on a pco.edge 4.2 sCMOS mounted on a Nikon Eclipse TE-2000 inverted microscope using 100× Ph3 objective (Plan Fluor, NA = 1.3). We focused on the solution phase of the sample instead of focusing on the surface of the glass slide to ensure imaging was representative of the whole solution and to avoid imaging vesicles that are known to grow from the surfaces of glass slides.[42]

Image Analysis

For Figure 1E, all vesicles larger than 5 μm visible in bright field were analysed, with a total of N = 49 across 12 brightfield micrographs and their 12 corresponding fluorescence micrographs.

Normalised Vesicle Brightness for fluorescence images

Intensity of encapsulated dye relative to background was measured in Fiji.[43] The mean gray scale value for approximately 5 $\times$ 5 μm rectangles inside (I_{in}) and outside (I_{bg}) the vesicles was determined using the *measure* tool. The normalized vesicle brightness was calculated by $(I_{\text{in}} - I_{\text{bg}})/I_{\text{bg}}$.

Normalized Transect Standard Deviation for brightfield images

Transects across vesicles T, including a background overlap on each side of the vesicle that is at least 10% of the total vesicle width on each side, were taken using the *line* tool and *plot profile* tool in Fiji.[43] The average of the first 10 pixels at the beginning of the transect was taken as the background value B. The transect T was then normalized against background T/B. The standard deviation σ of T/B was then reported as the Normalized Transect Standard Deviation.

Acknowledgement

L.H.S. is supported Australia Research Council Discovery Project DP180103204 awarded to M.V.K. A.W. is the recipient of an Australian Research Council Discovery Early Career Award (DE210100291). The authors would like to acknowledge and pay their respects to the Bedegal people, who are the traditional custodians of the land on which this research took place.

Supporting Information Available

Supporting figures S1 to S11 are provided in the supporting information document that can be found online at:

References

(1) Dzieciol, A. J.; Mann, S. Designs for life: protocell models in the laboratory. *Chem. Soc. Rev.* **2012**, *41*, 79–85.

(2) Rajamani, S.; Vlassov, A.; Benner, S.; Coombs, A.; Olasagasti, F.; Deamer, D. Lipid-assisted Synthesis of RNA-like Polymers from Mononucleotides. *Origins of Life and Evolution of Biospheres* **2008**, *38*, 57–74.

(3) Szathmáry, E.; Demeter, L. Group selection of early replicators and the origin of life. *Journal of Theoretical Biology* **1987**, *128*, 463–486.

(4) Chen, I. A. The Emergence of Competition Between Model Protocells. *Science* **2004**, *305*, 1474–1476.

(5) Szostak, J. W.; Bartel, D. P.; Luisi, P. L. Synthesizing life. *Nature* **2001**, *409*, 387–390.

(6) Apel, C. L.; Deamer, D. W.; Mautner, M. N. Self-assembled vesicles of monocarboxylic acids and alcohols: conditions for stability and for the encapsulation of biopolymers. *Biochimica et Biophysica Acta (BBA) - Biomembranes* **2002**, *1559*, 1–9.

(7) Rushdi, A. I.; Simoneit, B. R. Lipid formation by aqueous Fischer-Tropsch-type synthesis over a temperature range of 100 to 400 C. *Origins of Life and Evolution of the Biosphere* **2001**, *31*, 103–118.

(8) Meierhenrich, U.; Filippi, J.-J.; Meinert, C.; Vierling, P.; Dworkin, J. On the Origin of Primitive Cells: From Nutrient Intake to Elongation of Encapsulated Nucleotides. *Angewandte Chemie International Edition* **2010**, *49*, 3738–3750.

(9) Joshi, M.; Samanta, A.; Tripathy, G.; Rajamani, S. Formation and Stability of Prebiotically Relevant Vesicular Systems in Terrestrial Geothermal Environments. *Life* **2017**, *7*, 51.

(10) Morigaki, K.; Walde, P. Fatty acid vesicles. *Current Opinion in Colloid & Interface Science* **2007**, *12*, 75–80.

(11) Bernhardt, H. S.; Tate, W. P. Primordial soup or vinaigrette: did the RNA world evolve at acidic pH? *Biology Direct* **2012**, *7*, 4.

(12) Bonfio, C.; Russell, D. A.; Green, N. J.; Mariani, A.; Sutherland, J. D. Activation chemistry drives the emergence of functionalised protocells. *Chemical Science* **2020**, *11*, 10688–10697, Publisher: The Royal Society of Chemistry.

(13) Pinti, D. L. *Lectures in astrobiology*; Springer, 2005; pp 83–112.

(14) Maurer, S.; Deamer, D.; Boncella, J.; Monnard, P.-A. Chemical Evolution of Amphiphiles: Glycerol Monoacyl Derivatives Stabilize Plausible Prebiotic Membranes. *Astrobiology* **2009**, *9*, 979–987.

(15) Monnard, P.-A.; Deamer, D. W. *Methods in Enzymology*; Elsevier, 2003; Vol. 372; pp 133–151.

(16) Morigaki, K.; Walde, P.; Misran, M.; Robinson, B. H. Thermodynamic and kinetic stability. Properties of micelles and vesicles formed by the decanoic acid/decanoate system. *Colloids and Surfaces A: Physicochemical and Engineering Aspects* **2003**, *213*, 37–44.

(17) Namani, T.; Deamer, D. W. Stability of Model Membranes in Extreme Environments. *Origins of Life and Evolution of Biospheres* **2008**, *38*, 329–341.

(18) Milshteyn, D.; Damer, B.; Havig, J.; Deamer, D. Amphiphilic Compounds Assemble

into Membranous Vesicles in Hydrothermal Hot Spring Water but Not in Seawater. *Life* **2018**, *8*, 11.

(19) Laughlin, R. Equilibrium vesicles: fact or fiction? *Colloids and Surfaces A: Physicochemical and Engineering Aspects* **1997**, *128*, 27–38.

(20) Campbell, T. D.; Febrian, R.; McCarthy, J. T.; Kleinschmidt, H. E.; Forsythe, J. G.; Bracher, P. J. Prebiotic condensation through wet–dry cycling regulated by deliquescence. *Nature Communications* **2019**, *10*, 4508.

(21) Westall, F.; Hickman-Lewis, K.; Hinman, N.; Gautret, P.; Campbell, K.; Bréhéret, J.; Foucher, F.; Hubert, A.; Sorieul, S.; Dass, A.; Kee, T.; Georgelin, T.; Brack, A. A Hydrothermal-Sedimentary Context for the Origin of Life. *Astrobiology* **2018**, *18*, 259–293.

(22) Steller, L. H.; Nakamura, E.; Ota, T.; Sakaguchi, C.; Sharma, M.; Van Kranendonk, M. J. Boron Isotopes in the Puga Geothermal System, India, and Their Implications for the Habitat of Early Life. *Astrobiology* **2019**, *19*, 1459–1473.

(23) Van Kranendonk, M. J.; Baumgartner, R.; Djokic, T.; Ota, T.; Steller, L.; Garbe, U.; Nakamura, E. Elements for the Origin of Life on Land: A Deep-Time Perspective from the Pilbara Craton of Western Australia. *Astrobiology* **2021**, *21*, 39–59.

(24) Deamer, D. W.; Barchfeld, G. L. Encapsulation of macromolecules by lipid vesicles under simulated prebiotic conditions. *Journal of Molecular Evolution* **1982**, *18*, 203–206.

(25) Damer, B.; Deamer, D. Coupled Phases and Combinatorial Selection in Fluctuating Hydrothermal Pools: A Scenario to Guide Experimental Approaches to the Origin of Cellular Life. *Life* **2015**, *5*, 872–887.

(26) Sarkar, S.; Dagar, S.; Rajamani, S. Influence of Wet-dry Cycling on the Self-Assembly and Physicochemical Properties of Model Protocellular Membrane Systems. *ChemSystemsChem*

(27) Namani, T.; Walde, P. From decanoate micelles to decanoic acid/dodecylbenzenesulfonate vesicles. *Langmuir* **2005**, *21*, 6210–6219.

(28) Melchior, D. L.; Steim, J. M. Thermotropic Transitions in Biomembranes. *Annual Review of Biophysics and Bioengineering* **1976**, *5*, 205–238.

(29) Hargreaves, W. R.; Deamer, D. W. Liposomes from ionic, single-chain amphiphiles. *Biochemistry* **1978**, *17*, 3759–3768.

(30) Maurer, S. E.; Tølbøl Sørensen, K.; Iqbal, Z.; Nicholas, J.; Quirion, K.; Gioia, M.; Monnard, P.-A.; Hanczyc, M. M. Vesicle Self-Assembly of Monoalkyl Amphiphiles under the Effects of High Ionic Strength, Extreme pH, and High Temperature Environments. *Langmuir* **2018**, *34*, 15560–15568.

(31) Reeves, J. P.; Dowben, R. M. Formation and properties of thin-walled phospholipid vesicles. *Journal of Cellular Physiology* **1969**, *73*, 49–60.

(32) Zhang, H. Liposomes: methods and protocols. 2017.

(33) Maeda, H.; Eguchi, Y.; Suzuki, M. Hydrogen ion titration of oleic acid in aqueous media. *The Journal of Physical Chemistry* **1992**, *96*, 10487–10491.

(34) Mele, S.; Söderman, O.; Ljusberg-Wahrén, H.; Thuresson, K.; Monduzzi, M.; Nylander, T. Phase behavior in the biologically important oleic acid/sodium oleate/water system. *Chemistry and Physics of Lipids* **2018**, *211*, 30–36.

(35) Kindt, J. T.; Szostak, J. W.; Wang, A. Bulk Self-Assembly of Giant, Unilamellar Vesicles. *ACS Nano* **2020**, *14*, 14627–14634.

(36) Thomas, J. A.; Rana, F. The influence of environmental conditions, lipid composition, and phase behavior on the origin of cell membranes. *Origins of Life and Evolution of Biospheres* **2007**, *37*, 267–285.

(37) Luisi, P. L. Are Micelles and Vesicles Chemical Equilibrium Systems? *Journal of Chemical Education* **2001**, *78*, 380.

(38) Jordan, S. F.; Rammu, H.; Zheludev, I. N.; Hartley, A. M.; Maréchal, A.; Lane, N. Promotion of protocell self-assembly from mixed amphiphiles at the origin of life. *Nature ecology & evolution* **2019**, *3*, 1705–1714.

(39) Sarkar, S.; Das, S.; Dagar, S.; Joshi, M. P.; Mungi, C. V.; Sawant, A. A.; Patki, G. M.; Rajamani, S. Prebiological Membranes and Their Role in the Emergence of Early Cellular Life. *The Journal of Membrane Biology* **2020**, *253*, 589–608.

(40) Walde, P.; Ichikawa, S. Enzymes inside lipid vesicles: preparation, reactivity and applications. *Biomolecular engineering* **2001**, *18*, 143–177.

(41) Matsushita-Ishiodori, Y.; Hanczyc, M. M.; Wang, A.; Szostak, J. W.; Yomo, T. Using Imaging Flow Cytometry to Quantify and Optimize Giant Vesicle Production by Water-in-oil Emulsion Transfer Methods. *Langmuir* **2019**, *35*, 2375–2382.

(42) Morigaki, K.; Walde, P. Giant vesicle formation from oleic acid/sodium oleate on glass surfaces induced by adsorbed hydrocarbon molecules. *Langmuir* **2002**, *18*, 10509–10511.

(43) Schindelin, J. et al. Fiji: an open-source platform for biological-image analysis. *Nature Methods* **2012**, *9*, 676–682, Number: 7 Publisher: Nature Publishing Group.

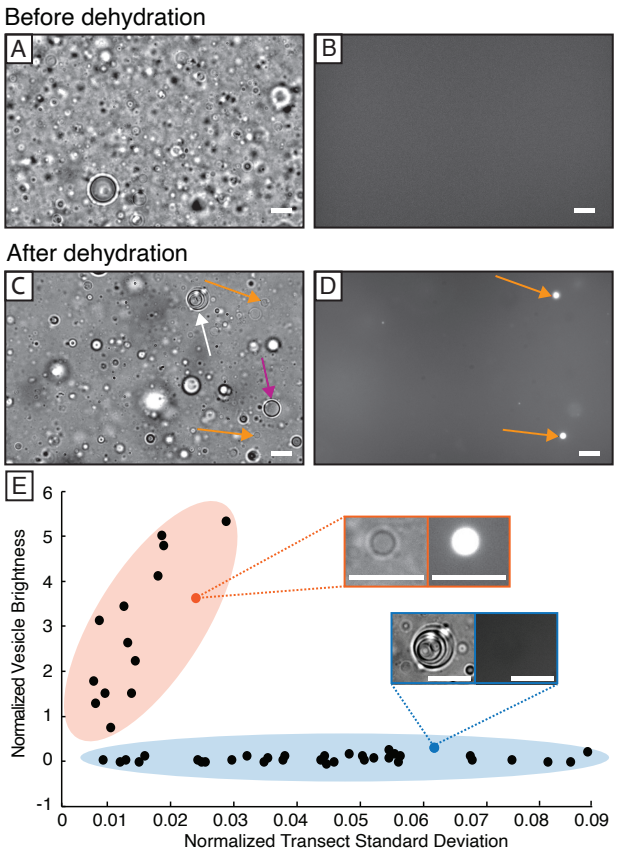

Figure 1: DA:GMD vesicles with RNA and QuantiFluor (RNA dye) in 1X PBS buffer (pH 7.4): A) The system before dehydration. Brightfield microscopy confirms that vesicles are present. B) Fluorescence microscopy shows that no encapsulation of the RNA has occurred. C) After one DR event vesicles are still present, including thin walled vesicles (orange arrows), multilamellar vesicles (white arrow) and thick-walled vesicles (pink arrow). D) Fluorescence microscopy reveals that enhanced RNA encapsulation (orange arrows) occurs only within thin-walled vesicles. E) After a single DR event, enhanced encapsulation occurred for some thin-walled vesicles. This graph depicts the normalized vesicle brightness, a proxy for amount of material encapsulated, against the standard deviation of a vesicle transect in bright field, a proxy for vesicle wall lipid density for $N = 49$ vesicles (see Methods and Fig. S2). Orange box outlines thin-walled vesicles (a normalised transect value > 0.03) and blue box outlines multi-walled vesicles (normalised transect value < 0.03). Scale bar represents 10 μm.

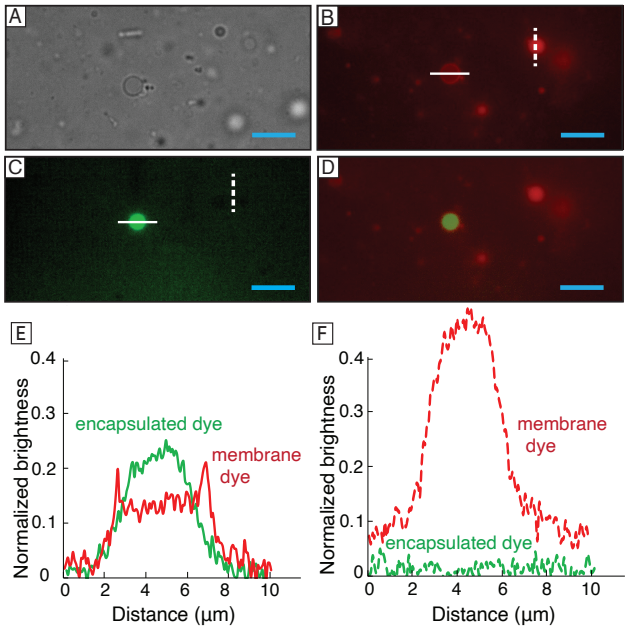

Figure 2: DA:GMD vesicles with pyranine as the encapsulation molecule in 1X PBS buffer (pH 7.4) after a single dehydration event: A) brightfield microscopy image of sample, B) Rhodamine B fluorescence channel shows that a mixture of vesicle types are present in the system after rehydration, including thin-walled (white solid line) and thick-walled vesicles (white dotted line) C) pyranine fluorescence channel D) composite image of Rhodamine B and pyranine channels E) gray-value transect of Rhodamine B (red) and encapsulated pyranine (green) demonstrating encapsulation within the thin-walled vesicle, compared to a F) a transect of a dense lipid droplet (white dotted line in panels B-C). See Methods for further details of image analysis. Scale bar in blue represents 10 μm. Additional examples of Rhodamine B/brightfield/Pyranine vesicle image sets demonstrating vesicle formation and encapsulation can be found in Fig. S3.

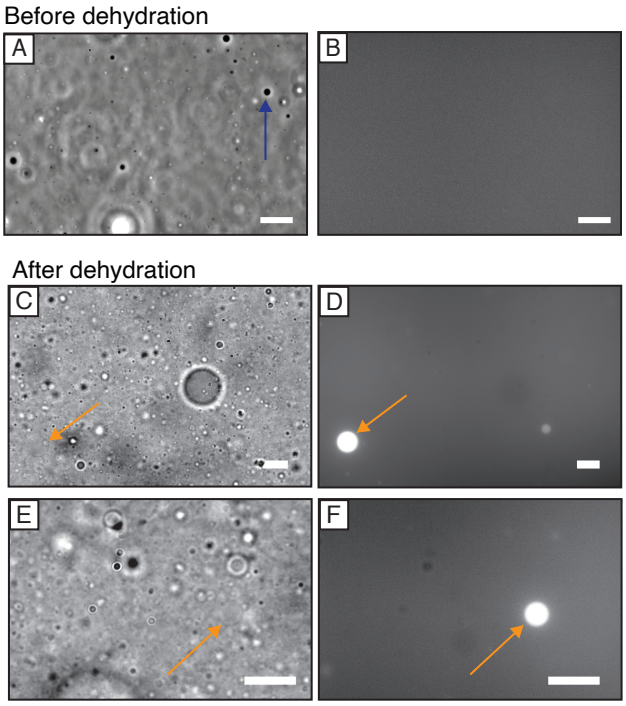

Figure 3: DA:GMD vesicles with RNA and QuantiFluor (RNA dye) in 10mM NaCl solution (pH 5.4). A) Before dehydration, the lipid forms droplets because the solution is below the apparent pK_a of the fatty acid (blue arrow). B) The solution exhibits homogeneous fluorescence indicating that RNA is evenly dispersed through the solution. C-F) One DR event has remodelled the lipid to form a wide range of vesicles, including thin-walled vesicles that show enhanced RNA encapsulation (orange arrows). Panels A, C, and E are brightfield optical micrographs, panels B, D, and F are fluorescence images. Scale bar represents 10 μm.

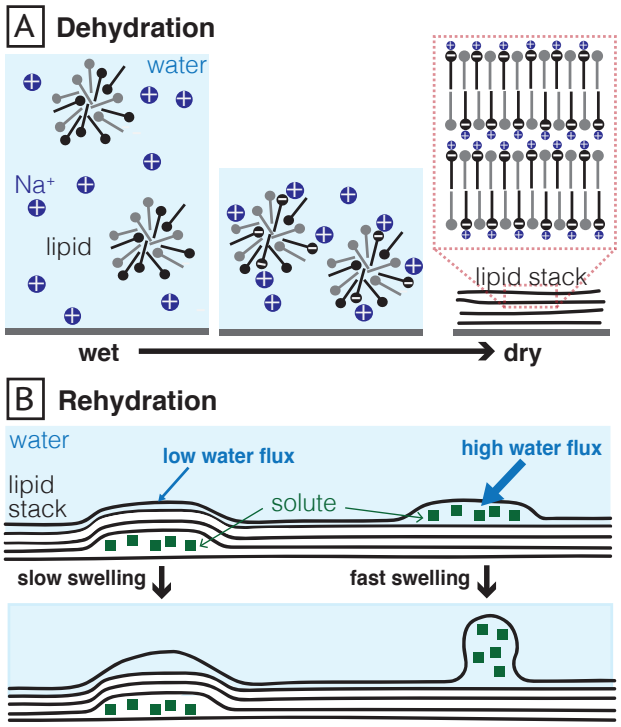

Figure 4: A) During dehydration, solutes such as sodium ions (blue) as well as aggregates of non-ionizable lipid (glycerol monodecanoate, gray) and ionizable lipid (decanoic acid, black) are concentrated. An increase in ionic strength leads to a decrease in decanoic pK_a, deprotonating the decanoic acid. These ionized groups can then interact with sodium cations and form pre-organized lipid layers. B) Rehydration preferentially swells pockets of solute molecules (green) that are bound by fewer bilayers.